5-2008

Targeting of Thyroid Hormone Receptor Variants to Aggresomes

Abigail Brunner
College of William and Mary

Targeting of Thyroid Hormone Receptor Variants to Aggresomes

A thesis submitted in partial fulfillment of the requirement
for the degree of Bachelors of Science in Biology from
The College of William and Mary

by

Abigail Maria Brunner

Williamsburg, VA
May 2008

Table of Contents

List of Figures

Abstract

The thyroid hormone receptor (TR) alters gene transcription in response to thyroid hormone (T_3). Our prior studies demonstrated that dominant negative variants, including the retroviral oncoprotein v-ErbA, mislocalize to the cytoplasm and sequester TR in foci suggestive of aggresomes. Formation of the aggresome is a cellular response to the accumulation of misfolded protein aggregates for turnover. Starting as mini-aggregates, they are transported along microtubule tracks to the microtubule organizing center (MTOC), where they disrupt vimentin intermediate filaments and recruit machinery for protein degradation. Viral particles also follow the same aggresomal pathway to facilitate replication and assembly. To test for association with aggresomes, HeLa cells were cotransfected with the aggresomal markers GFP-250 and GFP-170 and DsRed2-tagged v-ErbA. There was a strong colocalization between the aggresomal markers and v-ErbA, suggesting that they are both targeted to the same subcellular location. v-ErbA foci disrupt vimentin, further demonstrating their aggresome-like properties. Proteasome inhibition is known to induce aggresome formation; thus, the effect of treatment of v-ErbA-expressing cells with the proteasome inhibitor MG132 was assessed. Upon treatment, there was a significant increase in foci size. Additionally, treatment with the microtubule-disrupting drug nocodazole inhibited aggresome formation. Taken together, these studies provide evidence for targeting of the oncoprotein v-ErbA to aggresomes, which is most likely a mechanism for its turnover.

Introduction

Proper intracellular trafficking of proteins, especially between the nucleus and cytoplasm, is necessary for cellular function. Accordingly, protein mislocalization can lead to a number of diseases, especially cancer (Fabbro and Henderson, 2003). Protein mislocalization can be caused by mutation and alteration of the original amino acid sequence, resulting in misfolding and disruption of function. Thus, turnover of these proteins is necessary to prevent further cell damage. v-ErbA, a retroviral oncogenic derivative of the thyroid hormone receptor (TR), is an example of a mutant protein that has altered subcellular localization and interferes with its wild type derivative. This thesis research investigated a potential pathway for the turnover of the oncoprotein v-ErbA.

Protein folding and misfolding

Proper protein function requires correct folding and maintenance of a newly synthesized amino acid chain into its correct three-dimensional conformation (Johnston et al., 1998; Garcia-Mata et al., 1999; Wigley et al., 1999). However, this does not always occur. Misfolding can result from particular mutations, errors in translation or environmental stresses. Correctly folded proteins embed their hydrophobic side chains in the interior of the folded protein. When proteins are not folded correctly, they expose their hydrophobic domains and accumulate in the cytoplasm, leading to inappropriate associations with other misfolded proteins and aggregation. This accumulation of cytoplasmic aggregates has been

correlated with the pathogenesis of a number of diseases, including Parkinson's, Huntington's, and Alzheimer's disease (Ross and Poirer, 2004). Though a strong correlation exists between these diseases and the accumulation of cytoplasmic aggregates, the exact mechanism of causation is not known. In response to these potential consequences, cells have evolved mechanisms to deal with misfolded or unfolded proteins.

Mechanism of aggresome formation

Aggresome formation is a method of dealing with the accumulation of cytoplasmic aggregates of misfolded proteins. The main purpose of the aggresome is to sequester these aggregates in a localized area to facilitate their disposal. When small protein aggregates accumulate in the cytoplasm due to misfolding, they are recognized by dynein motors and transported in a minus-end direction to the microtubule organizing center (MTOC), coalescing into a large aggregate of loosely associated particles (Garcia-Mata et al., 1999) (Figure 1).

Once these aggregates have coalesced, the intermediate filament meshwork composed of vimentin is disrupted and collapses around the aggregated proteins to immobilize and contain them in this localized area (Johnston et al., 1998; Garcia-Mata et al., 1999). At this point, chaperone proteins, proteasome machinery and ubiquitin are recruited to help degrade these proteins. Ubiquitination is not a requirement for proteasome-mediated degradation; ubiquitin-independent proteasome degradation can also occur in the aggresome (Garcia-Mata et al., 1999).

(a)

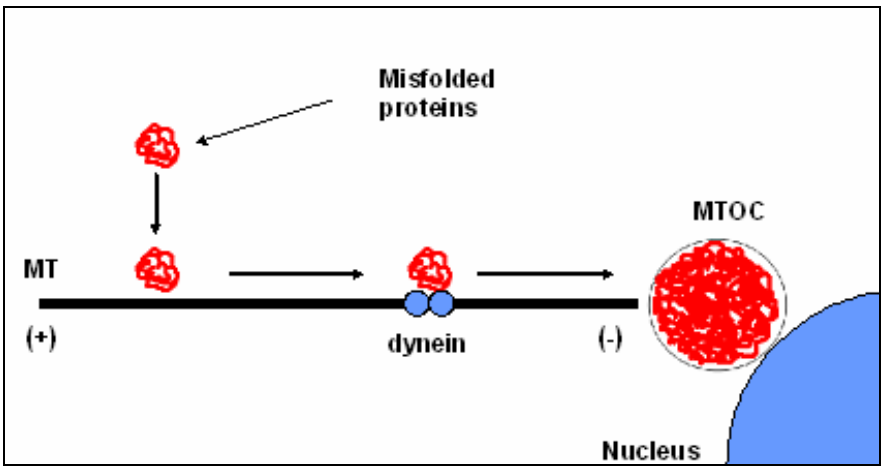

(b)

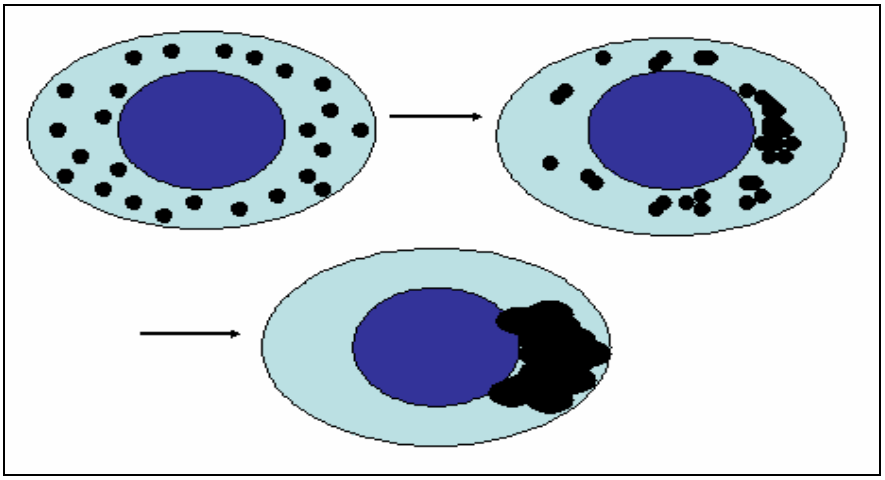

Figure 1: Aggresome formation

(a) Sequestration and coalescence of aggregates of misfolded proteins at the microtubule organizing center (MTOC), mediated by dynein motor proteins.
(b) Dynamics of aggresome formation. Dispersed aggregates fuse together and coalesce at the MTOC to form the aggresome.

Despite the recruitment of chaperones and proteasomes, protein aggregates are only degraded to a limited extent (Garcia-Mata et al., 2002). However, the aggresome also induces autophagy, which engulfs these aggregates and directs them to the lysosome for degradation (Fortun et al., 2003). This system is a lot more efficient in the disposal of protein aggregates because these coalesced aggregates can be engulfed simultaneously due to their wholesale sequestration in the cell.

Degradation and clearance mechanisms induced by aggresome formation

One mechanism of protein turnover is the ubiquitin-proteasome system. In this cellular process, the protein of interest is linked to a number of ubiquitin molecules, which is a signal for the protein to be directed to the proteasome (Wigley et al., 1999; Fabunmi et al., 2000; Ross and Poirier, 2004). The most common proteasome complex in eukaryotic cells is the 26S proteasome, which consists of a 20S core and two 19S regulatory caps. The 19S caps bind ubiquitinated proteins, remove ubiquitin, and unfold the substrate so that it can be translocated into the 20S core, which is the site of proteolysis. The proteolytic subunits in the 20S core cleave peptide bonds between amino acids, resulting in short peptide fragments. Proteolytic activity can be chymotrypsin-like, trypsin-like, and peptidyl-glutamyl peptide-hydrolyzing (PHGH)-like, depending on the nature of the amino acid side-chains in the substrate (Wojcik et al., 1996; Lee and Goldberg, 1998).

Autophagy is another mechanism of protein turnover activated by cellular stress, especially the accumulation of misfolded proteins. The autophagic pathway allows isolation membranes

to engulf a portion of the cytoplasm containing the substrate of interest (Klionsky, 2005). Isolation membranes mature into autophagosomes, which fuse with lysosomes and undergo degradation via acid hydrolases (Mortimore et al., 1996).

Effects of the aggresome on cell components

Although the aggresome triggers a disruption of intermediate filaments (Johnston et al., 1998; Garcia-Mata et al., 1999), it does not appear to disrupt any other components of the cytoskeleton; the microfilaments and microtubules are not disturbed (Garcia-Mata et al., 1999; Muchowski et al., 2000). Additionally, the structure and function of a number of organelles, including the endoplasmic reticulum, Golgi, and lysosomes do not appear to be altered. While the function of the mitochondria is not compromised, they have been shown to migrate to the aggresome (Mittal et al., 2007). A possible explanation for mitochondrial migration is to facilitate the supply of ATP to the chaperone proteins and proteasomes.

Aggresome discovery

The aggresome was first identified in a study that examined the cellular responses to the accumulation of aggregates formed by a cystic fibrosis transmembrane regulator (CFTR) mutant with the deletion of phenylalanine 508 (ΔF508) (Johnston et al., 1999). The wild-type transmembrane protein serves as a chloride channel. When CFTR does not fold correctly, it cannot be transported properly to the cell membrane and cannot carry out its function, resulting in cystic fibrosis. In the presence of proteasome inhibitors, misfolded CFTR

coalesced into a large aggregate at the MTOC, which was named the aggresome. This novel structure contained ubiquitin, disrupted the intermediate filament meshwork composed of vimentin, and required intact microtubules. The same results were obtained in response to an accumulation of the misfolded integral membrane protein presenilin-1 (PS1), which is associated with Alzheimer's disease, suggesting that the aggresome is a general cellular response to the aggregation of misfolded protein.

Other aggresome-forming mutant proteins

A number of additional mutant proteins have been shown to follow the aggresome formation pathway and possess aggresomal characteristics. The vast majority of these aggregate-prone proteins are associated with disease states, especially neurodegenerative diseases. For example, aggresome-forming mutants of huntingtin (Lin et al., 2001; Muchowski et al., 2002), α-synuclein (Masliah et al. 2000), and opsin (Saliba et al., 2002) are correlated with Huntington's disease, Parkinson's disease, and Retinitis pigmentosa, respectively. Because of the high degree of correlation between aggresome formation and pathogenesis, it has been questioned whether the aggresome contributes to pathogenesis or protects cells from its consequences. Because most aggresomal research has been conducted in cells grown in culture, this question cannot be answered directly. However, studies in transgenic mice have suggested that there is a strong link between aggresome formation and neurodegeneration (Lin et al., 2001). Regardless, pathogenicity seems to be caused more by the lack of functional protein than the aggresome itself.

Aggresome markers

In addition to studying aggresomes formed by naturally occurring proteins, synthetic protein constructs have also been developed that mimic aggresome formation. These model systems are useful for characterizing aggresome composition, mechanisms involved in aggresome formation, and cellular responses to the aggresome. Additionally, these synthetic constructs are used as aggresomal markers, serving as reference points of subcellular localization to other potential aggresome-forming proteins. The aggresomal markers GFP-250 and GFP-170 were used extensively in this thesis research.

GFP-250

The aggresomal marker GFP-250 is composed of green fluorescent protein (GFP) fused at its C-terminus to the first 250 amino acids of the protein p115 (Garcia-Mata et al., 1999). The full length p115 is 959 amino acids long and is involved in the transport of cargo from the ER to the Golgi, specifically involved in the docking and fusion of cargo to the Golgi membrane (Nelson, et al. 1998). While the full length protein localizes to the Golgi complex, the truncated GFP-250 fusion protein aggregates into a single coalesced structure at the MTOC, displaying aggresomal characteristics (Garcia-Mata et al., 1999). Aggresome formation does not require proteasome inhibition. This truncated protein construct is aggregation-prone because the first 250 amino acids of p115 contain many hydrophobic side chains and cannot fold properly.

In concordance with other aggresome-forming proteins, GFP-250 aggresomes require microtubules for their formation, reorganize vimentin, and recruit chaperones and proteasomes; however, they do not show evidence of ubiquitination.

GFP-170

The aggresomal marker GFP-170 is composed of GFP fused to amino acids 566-1375 of the Golgi Complex Protein (GCP)-170, which is also known as golgin-160 (Fu et al., 2005). Truncation of this protein makes it aggregation-prone. While the specific function of GCP170 is poorly understood, it has been suggested that the protein plays a role in Golgi fragmentation during apoptosis (Hicks and Machamer 2002). The full-length GCP170 is localized to the Golgi, but the truncated GFP170 forms large ribbon-like aggregates at the MTOC (Fu et al., 2005). Therefore, the cytoplasmic aggregates formed by GFP-170 and GFP-250 differ in morphology. In addition to the cytoplasmic aggregates, GFP-170 also forms punctate foci in the nucleus. The exact mechanism of how GFP-170 enters the nucleus is not known. However, it has been speculated that the protein contains an unidentified nuclear localization signal.

Alternate use of aggresomal pathway- viral replication and assembly

Interestingly, in addition to waste disposal systems for the accumulation of aggregated proteins, aggresomes can also function as sites for viral replication and assembly (Wileman 2006). These two processes often take place in localized areas within the cell, which are

referred to as viral factories (Wileman et al., 2001). Concentration of essential viral components, especially genetic material and structural proteins, facilitates assembly. In order to sequester these necessary components, viruses exploit the same aggresomal pathway used to sequester misfolded proteins for their disposal (Figure 2).

In addition to recognizing protein aggregates, dynein motors can also recognize viral components, which are transported along microtubules to the MTOC, serving as a scaffold for replication and assembly (Wileman 2006). Consistent with the responses triggered by aggregated misfolded proteins, viral factories reorganize vimentin to contain these viral components and exclude host proteins. Additionally, viral factories recruit chaperone proteins, ubiquitin and mitochondria. Furthermore, virus components can resist autophagy-mediated disposal by surviving harsh acidic and proteolytic conditions in the lysosome (Nozawa et al., 2004).

In summary, aggresomes are both sites for turnover of misfolded proteins and for viral replication and assembly. In this thesis research, these characteristics were further explored by investigating the association of a viral oncoprotein with aggresomes.

v-ErbA and the Avian Erythroblastosis Virus

v-ErbA, the focus of this research, is an oncogenic derivative of TRα1 (c-ErbA), carried by the avian erythroblastosis virus (AEV) (Thormeyer and Baniahmad, 1999). The thyroid hormone receptor (TR) is a type II nuclear hormone receptor, which binds directly to DNA to

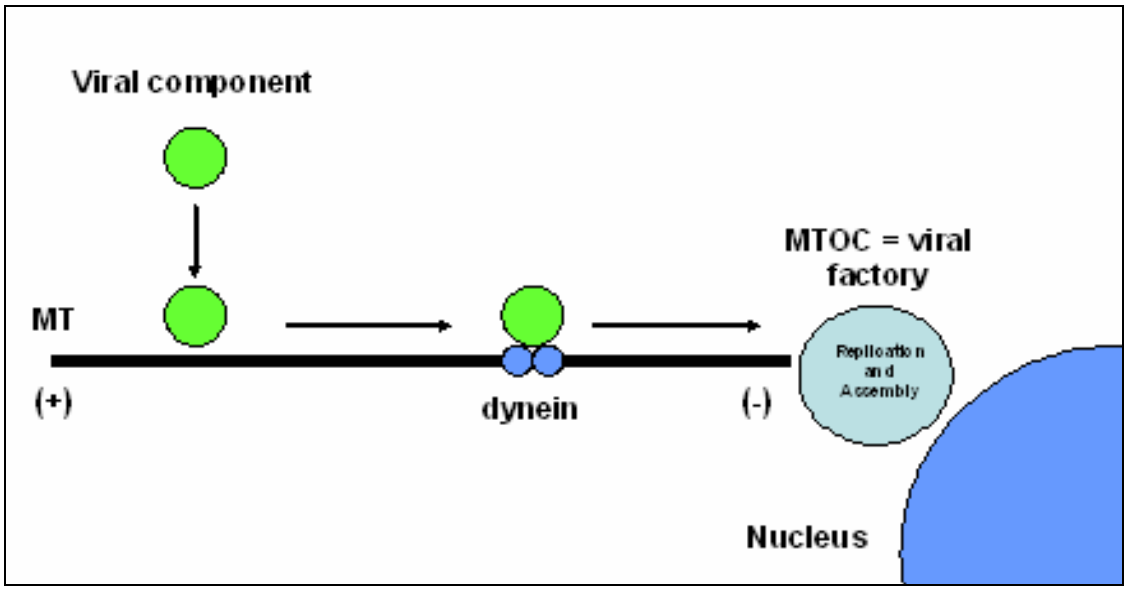

Figure 2: Alternate use of aggresomal pathway for viral replication and assembly

Replication and assembly of viruses take place in localized areas within the cell, which are referred to as viral factories. Concentration of essential viral components, especially genetic material and structural proteins, facilitates assembly. In order to sequester these necessary components, viruses exploit the same aggresomal pathway used to sequester misfolded proteins for their disposal. In addition to recognizing protein aggregates, dynein motors can also recognize viral components, which are transported along microtubules to the MTOC, serving as a scaffold for replication and assembly.

alter target gene transcription in response to the presence or absence of thyroid hormone (T_3) (Nagl et al., 1995). When bound to T_3, it can activate transcription of genes involved in mammalian and avian homeostasis, development, and metabolism. In the absence of T_3, TR acts a repressor of these genes. Three out of the four isoforms of TR, TRα1, TRβ1, and TRβ2 can activate transcription in response to T_3 (Bunn et al., 2001).

AEV causes erythroleukemia and sarcomas in chickens (Braliou et al., 2001). v-ErbA acts as a repressor of T_3-responsive genes, contributing to the transformation of erythroblasts by preventing cell differentiation and promoting sustained cell proliferation.
The oncoprotein contains 13 amino acid substitutions, deletions in the amino and carboxyl-termini, and contains the Gag portion of the retrovirus fused to its N-terminus (DeLong et al., 2004). Gag proteins play a role in the formation of the viral capsid. Two of the point mutations are in the DNA binding domain and nine of them are in the ligand binding domain (Figure 3). Because v-ErbA is highly mutated in its ligand binding domain, it is unable to bind T_3; however, the oncoprotein is still able to bind DNA and overlapping thyroid hormone response elements, but not with the same affinity.

In addition to v-ErbA, AEV also encodes the oncoprotein v-ErbB, which is a highly mutated form of the epidermal growth factor receptor (Thormeyer and Baniahmad, 1999). These two oncoproteins are overproduced in infected avian cells. Together, v-ErbA and v-ErbB can transform cells through the transcriptional repression of genes involved in differentiation and cell cycle checkpoints.

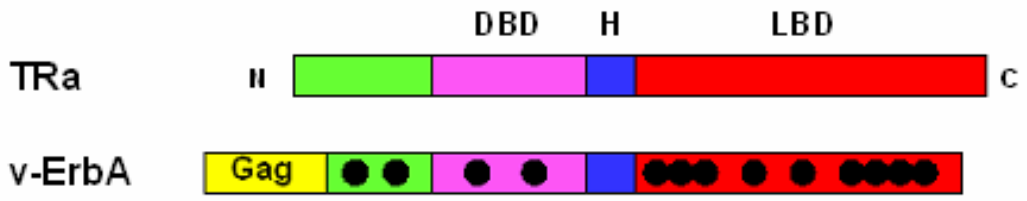

Figure 3: Oncogenic conversion of TRα to v-ErbA

v-ErbA contains 13 amino acid substitutions (black circles), deletions in the amino and carboxyl-termini, and contains the Gag (yellow) portion of the retrovirus fused to its N-terminus (green). Two of the point mutations are in the DNA binding domain (DBD, purple) and nine of them are in the ligand binding domain (LBD, red). H, hinge region (blue).

Role of v-ErbA in oncogenesis/dominant negative activity

v-ErbA can contribute to oncogenesis in a number of ways. First, it competes with TR for T_3-responsive DNA elements in the promoter region that aid in the transcription of T_3-responsive genes (Bonamy et al., 2005). Second, v-ErbA competes with TR for auxiliary factors (such as retinoid X receptor) and cofactors that promote T_3-mediated transcription. Third, v-ErbA dimerizes with TR and sequesters it in cytoplasmic foci.

Though TR shuttles between the nucleus and cytoplasm, it localizes primarily to the nucleus (Bunn et al., 2001). The physiological reason for the nucleocytoplasmic shuttling of TR is poorly understood. v-ErbA also shuttles between the nucleus and cytoplasm, but it has a significantly greater cytoplasmic localization than its homolog, TRα1 (DeLong et al., 2004). While TRα1 exhibits a mostly diffuse distribution throughout the nucleus, v-ErbA accumulates in cytoplasmic foci. Additionally, the oncoprotein exhibits a different mode of nuclear export in comparison to TRα1 (DeLong et al., 2004). Prior research has shown that v-ErbA exits the nucleus by a CRM1-dependent nuclear export pathway, primarily mediated by the acquisition of Gag sequence on the protein, which contains a nuclear export sequence. TRα1 is not solely dependent on CRM1 for nuclear export (Grespin et al., 2008). These findings suggest that differential cellular localization plays an important role in oncogenesis.

Specific Aims of Research

The overall objective of this thesis research was to determine whether the cytoplasmic foci formed by v-ErbA are a result of targeting to aggresomes. To this end, whether v-ErbA colocalized with aggresomal markers and possessed defining aggresomal characteristics was investigated. The following questions were addressed:

1. Does v-ErbA colocalize with aggresomal markers?
2. Is the formation of v-ErbA foci microtubule dependent?
3. Does proteasome inhibition enhance the size of v-ErbA foci?
4. Do v-ErbA foci disrupt vimentin intermediate filaments?

Materials and Methods

Plasmids

All plasmids used in this study encode fluorescently-tagged fusion proteins, in order to analyze the subcellular distribution of the proteins of interest. The GFP-250 and GFP-170 plasmids were gifts from E. Sztul (University of Alabama). GFP-250 was constructed by subcloning the PCR product of p115 cDNA into the enhanced green fluorescent protein (EGFP) expression vector pEGFP-C2 (Garcia-Mata et al., 1999). The GFP-170 plasmid expresses an EGFP- tagged portion of GCP-170 (Fu et al., 2005). The subcloning of v-ErbA into the GFP and DsRed2 vectors was conducted by other researchers in Dr. Allison's laboratory (Bunn et al, 2001; Bonamy et al., 2005). These plasmids were amplified in *E.coli* DH5α cells and purified using a Qiagen midi-prep kit according to the manufacturer's instructions. DNA yield was quantified using a Nanodrop ND-1000 full spectrum UV/Vis Spectrophotometer (NanoDrop Technologies).

GFP and DsRed2 are both naturally fluorescent proteins. GFP is derived from the jellyfish *Aequorea victoria* (Tsien, 1998). The protein has a major excitation peak at 395 nm (blue light), resulting in emission of green light. DsRed2 is a variant of DsRed, which is a red fluorescent protein derived from the coral *Discosoma* (Campbell et al., 2002). The DsRed2 protein has an excitation peak of 558 nm (green light), resulting in the emission of red light.

Cell culture, transfections, and drug treatments

Transfection experiments were performed in order to introduce plasmid DNA encoding fluorescently-tagged aggresomal markers and v-ErbA into HeLa human cells (Figure 4). After transfection, plasmid DNA was transcribed and translated within the cell into fluorescently-tagged proteins and their subcellular localization was observed by fluorescence microscopy. GFP-250, GFP-170, GFP-v-ErbA, and DsRed2-v-ErbA expression vectors were transfected into HeLa cells. In single transfections, only one type of plasmid was introduced into a cell (Figure 4a). In cotransfections, two plasmid DNA constructs were introduced into a cell and expressed simultaneously in order to test for colocalization to the same region within the cell (Figure 4b).

Cell culture was carried out in a Class II Biosafety Cabinet (Labconco). HeLa cells (human cervix epithelioid carcinoma; ATCC CCL-2) were grown and maintained at 37ºC and 5% CO_2 in Minimum Essential Medium (Gibco) with 10% fetal bovine serum (FBS) (Invitrogen) and penicillin-streptomycin antibiotics (100 U/mL penicillin and 100 µg/mL streptomycin) in a sterile large ($75cm^3$) filter-cap flask (NUNC Brand Products).

In preparation for transfection, cells were removed from the filter-cap flask by incubating them in 2 mL of chilled 0.25% trypsin solution for approximately 2 minutes. The trypsin was removed and the cells were incubated for another 5 minutes at 37ºC. After resuspension in HeLa media, 2 mL of growth medium containing 1-3 X 10^5 cells per well was added to each

(a) Single transfection **(b) Cotransfection**

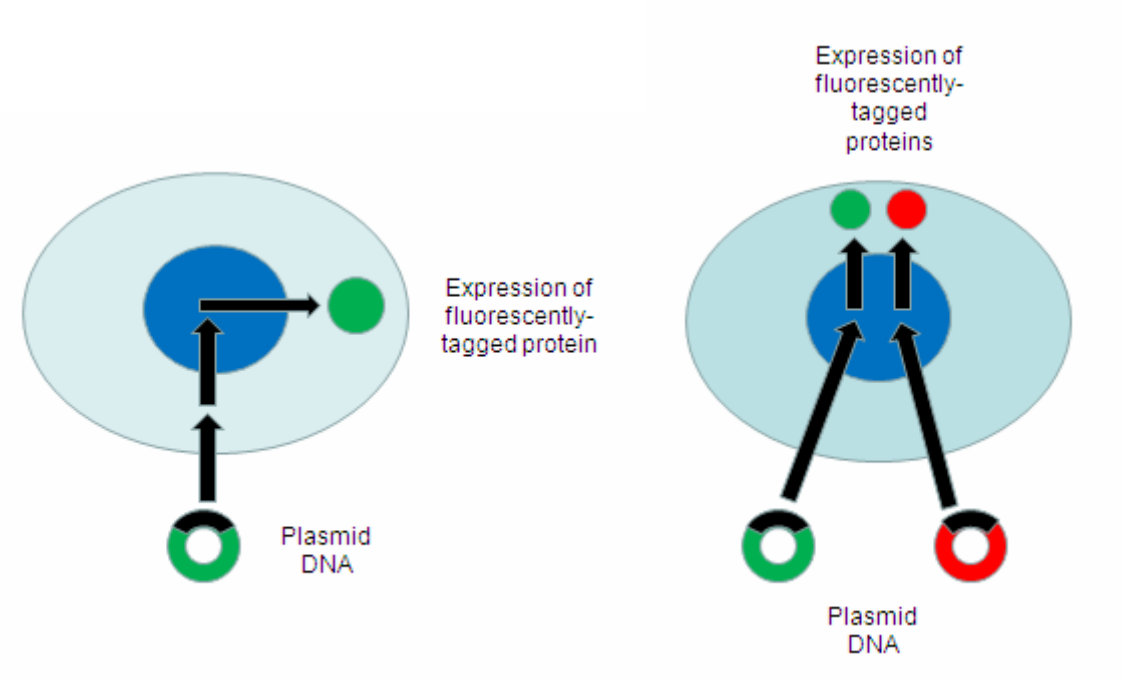

Figure 4: Transfection and cotransfection

Transfection experiments were performed in order to introduce plasmid DNA encoding fluorescently-tagged aggresomal markers and v-ErbA into HeLa cells. After transfection, plasmid DNA was transcribed and translated into fluorescently-tagged proteins and their subcellular localization was observed by fluorescence microscopy. GFP-250, GFP-170, GFP-v-ErbA, and DsRed2-v-ErbA expression vectors were transfected into HeLa cells. In single transfections, only one type of plasmid was introduced into a cell **(a)**. In cotransfections, two plasmid DNA constructs were introduced into a cell and expressed simultaneously in order to test for colocalization to the same region within the cell **(b)**.

well of a 6-well plate with glass coverslips (Fisher) and incubated at 37ºC for approximately 24 hours, reaching a confluency of about 50-60%.

Lipofectamine Reagent (Invitrogen) was used to perform transfections. For single transfections, 2 µg of plasmid was diluted in Opti-MEM reduced serum media (Gibco) for a total volume of 100µL. For cotransfections, 1 µg of each plasmid (2 µg total) was diluted in Opti-MEM. A second 100µL solution was prepared with 10µL of Lipofectamine Reagent and 90µL of Opti-MEM. The two solutions were combined (200 µL total) and incubated at room temperature for 15 minutes. After incubation, 800 µL of Opti-MEM was added to the 200 µL solution of DNA-liposome complex. This 1 mL solution of diluted DNA-liposome complex was added to each seeded coverslip in the 6-well plate. The transfected cells were incubated at 37ºC for 16-20 hours. The Opti-MEM was removed from the cells and replaced with 2 mL of complete media. Cells were fixed and stained 24-48 hours post-transfection to be analyzed by fluorescence microscopy. The time period between transfection and fixation depended on the experiment.

When testing the effect of treatment with the proteasome-inhibiting drug MG132 (Sigma) and the microtubule-disrupting drug nocodazole (Sigma), 2 µL of MG132 solution, nocodazole solution, or DMSO (vehicle control) were added to each well after media replacement. Both MG132 and nocodazole were dissolved in DMSO at a concentration of 10 mg/mL. The treated cells were incubated for 16-20 hours to allow sufficient proteasome inhibition and microtubule depolymerization.

Fixation, immunofluorescence staining, and processing of cells for imaging

24-48 hours after transfection, media was removed from cells. Cells were washed 3 times for 15 seconds in 2 mL per well with Dulbecco's Phosphate-Buffered Saline (D-PBS: 0.10g KCl, 0.10g KH_2PO_4, 4.00g NaCl, and 1.08g $Na_2HPO_4 \cdot 7H_2O$) for a solution of 500 mL). For fixation, cells were incubated in a 3.7% formaldehyde solution with D-PBS for 10 minutes. After fixation, the formaldehyde solution was removed and the cells were washed 3 times in D-PBS for 5 minutes.

Cells being processed for immunofluorescence staining were permeabilized for 5 minutes in a 0.2% Triton-X-100 solution diluted with D-PBS. Coverslips were inverted onto 30 µL of a diluted antibody solution with 1.5% normal goat sera and D-PBS. A 1:200 dilution was used for the monoclonal Cy3-conjugated anti-vimentin antibody (Sigma). The cells were incubated in the antibody for 1 hour in the dark in a humidified chamber. The humidified chamber consisted of a storage container lined with moist paper towels. The 30 µL of antibody solution and coverslips were placed on parafilm, which was placed on top of the moist paper towels.

Because the Cy3-conjugated vimentin antibody was labeled, incubation with a labeled secondary antibody was not necessary. After incubation with the labeled primary antibody, cells were washed 3 times in D-PBS for 5 minutes in the original 6-well plate. The washes

were performed on a rotating table, allowing antibody that was non-specifically bound to be washed off the coverslip.

After the washes, coverslips were inverted and mounted onto slides with 8 µL of GelMount with DAPI (0.5 mg/L). Cells that were not stained with antibody were mounted onto slides and stained with DAPI immediately after the 3 post-fixation washes. All of the mounted slides were viewed by fluorescence microscopy.

Fluorescence microscopy

Prepared slides were analyzed with an Olympus Fluorescence Microscope. Three separate filters were used to visualize the DAPI-stained nucleus (UV for blue fluorescence), GFP-tagged protein (blue light for green fluorescence), and both DsRed2-tagged protein and Cy3-conjugated antibody (green light for red fluorescence). This allowed for the determination of subcellular localization in relation to the nucleus. Cells were photographed with a Cooke SensiCamQE digital camera. IP Lab software and Adobe Photoshop CS were used to normalize, pseudocolor, and layer the captured images.

Cell scoring and statistical analysis

Three trials of colocalization assays between DsRed2-v-ErbA and GFP-250 were performed, with at least 100 cells analyzed per trial. Transfected cells were categorized into 3 different groups: total, partial, and no colocalization. Two trials of treatment of GFP-v-ErbA with

MG132 and nocodazole were conducted, with at least 100 cells analyzed per trial. Aggregate size in the transfected and treated cells was categorized into 3 different groups: diffuse, small, or large aggregates. Three trials of colocalization between GFP-v-ErbA and the anti-vimentin antibody were performed, with greater than 100 cells analyzed per trial.

Once cells were counted in the drug treatment experiments, results were tested for statistical significance using SPSS (v. 16). Data were analyzed for frequency distribution using a Chi-Square test; a p-value of 0.001 or less was considered significant.

Results

v-ErbA colocalizes with aggresomal markers

Prior studies had shown that v-ErbA has a mainly cytoplasmic distribution, localized in punctate foci (Bunn et al., 2001; Bonamy et al., 2005). To determine whether v-ErbA associates with aggresomes, the distribution of v-ErbA was analyzed by transfection assays with fluorescently-tagged fusion proteins.

Before testing for colocalization between v-ErbA and aggresomal markers, the cellular localizations of DsRed2-v-ErbA, GFP-v-ErbA, GFP-170, and GFP-250 were observed individually in HeLa cells. Consistent with prior studies (Garcia-Mata et al., 1999), GFP-250 formed entirely cytoplasmic aggregates (Figure 5a and b). After about 48 hours post-transfection, some of the GFP-250-expressing cells displayed a single coalesced juxtanuclear aggregate that was spherical in shape, while other cells displayed a number of smaller aggregates throughout the cytoplasm. These smaller aggregates were not evenly dispersed or uniform in size; aggregates were more heavily concentrated near one side of the nucleus. The localization and variation in size of these aggregates suggests that smaller aggregates fused together and were in the process of being transported to the microtubule organizing center (MTOC). Also consistent with prior studies (Fu et al., 2005), GFP-170 formed both nuclear and cytoplasmic aggregates after observing the protein's distribution 48 hours after transfection (Figure 5c and d). The protein localized to punctate foci in the nucleus and in

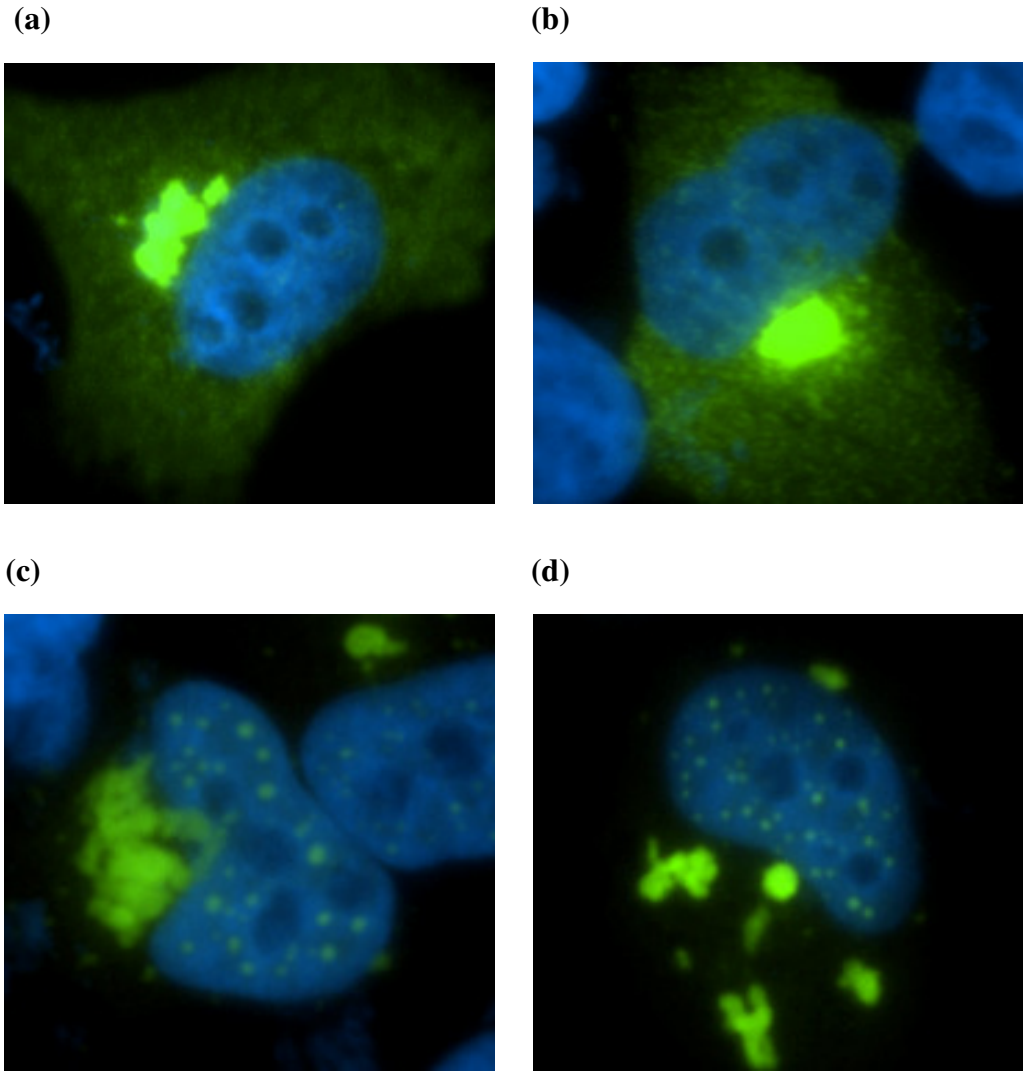

Figure 5: Subcellular localization of the aggresomal markers GFP-250 and GFP-170 (48 hours post-transfection)

(a) and (b) GFP-250 forms cytoplasmic aggregates. Some of the GFP-250-expressing cells displayed a single coalesced juxtanuclear aggregate that was spherical in shape, while other cells displayed a number of smaller aggregates throughout the cytoplasm. Nuclei were stained with DAPI (blue).
(c) and (d) GFP-170 forms nuclear and cytoplasmic aggregates. The protein localized to punctate foci in the nucleus and formed large ribbon-like aggregates, proximal to the nucleus. Nuclei were stained with DAPI (blue).

contrast with GFP-250, formed large ribbon-like aggregates, instead of spherical aggregates, proximal to the nucleus.

Forty-eight hours after transfection, GFP and DsRed2-tagged-v-ErbA formed almost entirely cytoplasmic aggregates; there was a range of cytoplasmic distribution (not shown). Some v-ErbA expressing cells contained a single coalesced juxtanuclear aggregate with a ribbon-like and elongated morphology (Figure 6a), similar to the cytoplasmic aggregates formed by GFP-170, while other cells contained smaller and more dispersed aggregates (Figure 6b), and some cells had an entirely diffuse cytoplasmic distribution. As in the aggresomal markers, the cytoplasmic foci formed by v-ErbA were not uniform in size or evenly dispersed, suggesting that they were in the process of aggresome formation. The cellular distribution pattern of v-ErbA was similar to the distribution patterns of the aggresomal marker GFP-250 and the cytoplasmic aggregates of GFP-170.

To investigate whether or not the foci formed by v-ErbA colocalized with aggresomal markers, HeLa cells were cotransfected with GFP-tagged aggresomal markers (GFP-170 and GFP-250) and DsRed2-tagged v-ErbA and their subcellular localizations were observed. Forty-eight hours after transfection, DsRed2-v-ErbA and GFP-250 completely colocalized in 59 ± 4% of cells and partially colocalized in 38 ± 4% of cells (n=3 replicate transfections, 313 cells scored) (Figure 7, Figure 8). These results strongly suggest that DsRed2-v-ErbA and GFP-250 are targeted to the same subcellular location, despite their slight differences in morphology.

(a) **(b)**

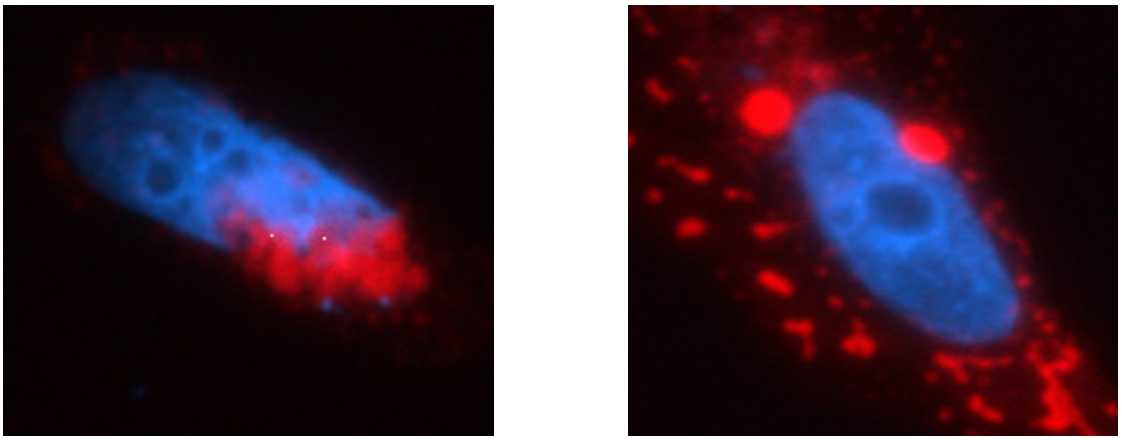

Figure 6: Subcellular distribution of DsRed2 v-ErbA (48 hours post-transfection)

(a) DsRed2-v-ErbA-expressing cell containing a single coalesced juxtanuclear aggregate with a ribbon-like and elongated morphology, similar to the cytoplasmic aggregates formed by GFP-170 (See Figure 5c). Nuclei were stained with DAPI (blue).
(b) DsRed2-v-ErbA-expressing cell containing smaller and more dispersed aggregates. Nuclei were stained with DAPI (blue).

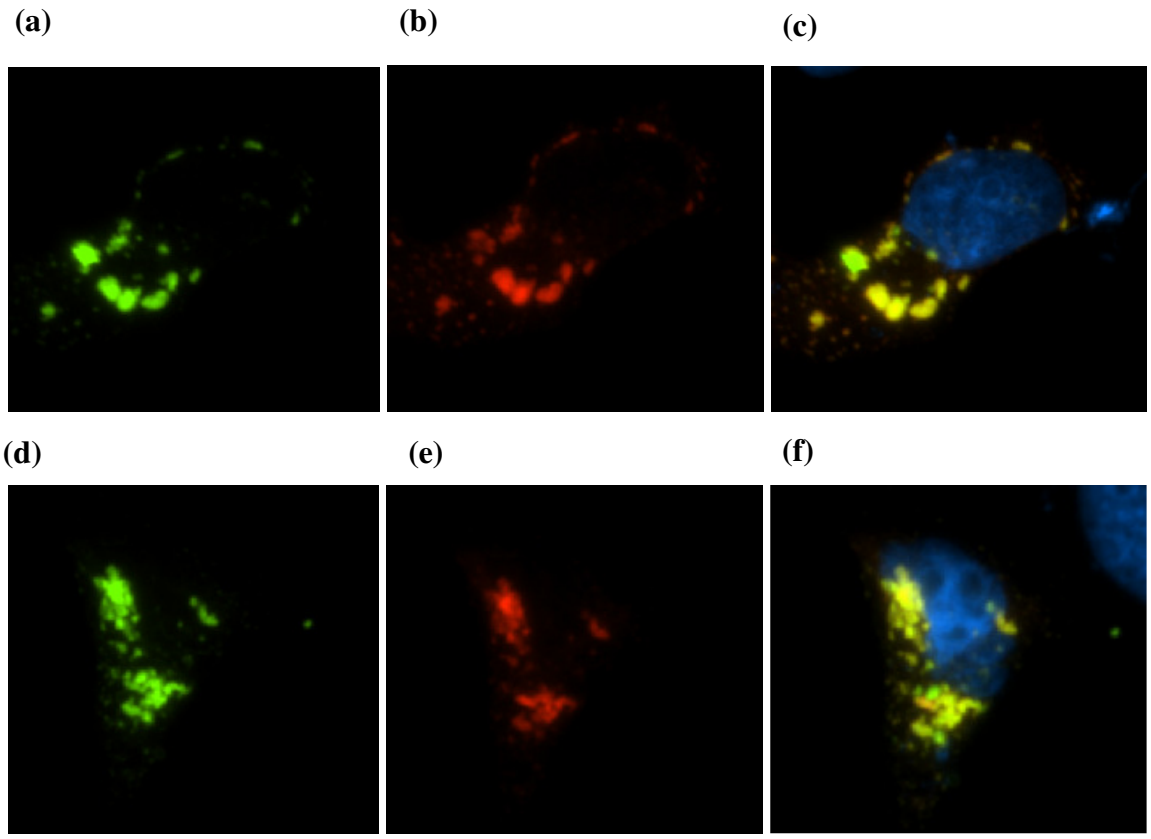

Figure 7: Colocalization of the aggresomal marker GFP-250 and DsRed2-v-ErbA (48 hours post-transfection)

(a) and (d) Subcellular distribution of GFP-250 (green)
(b) and (e) Subcellular distribution of DsRed2-v-ErbA (red)
(c) and (f) Merge of GFP-250 and DsRed2-v-ErbA. Yellow indicates colocalization between GFP-250 and DsRed2-v-ErbA. Nuclei were stained with DAPI (blue).

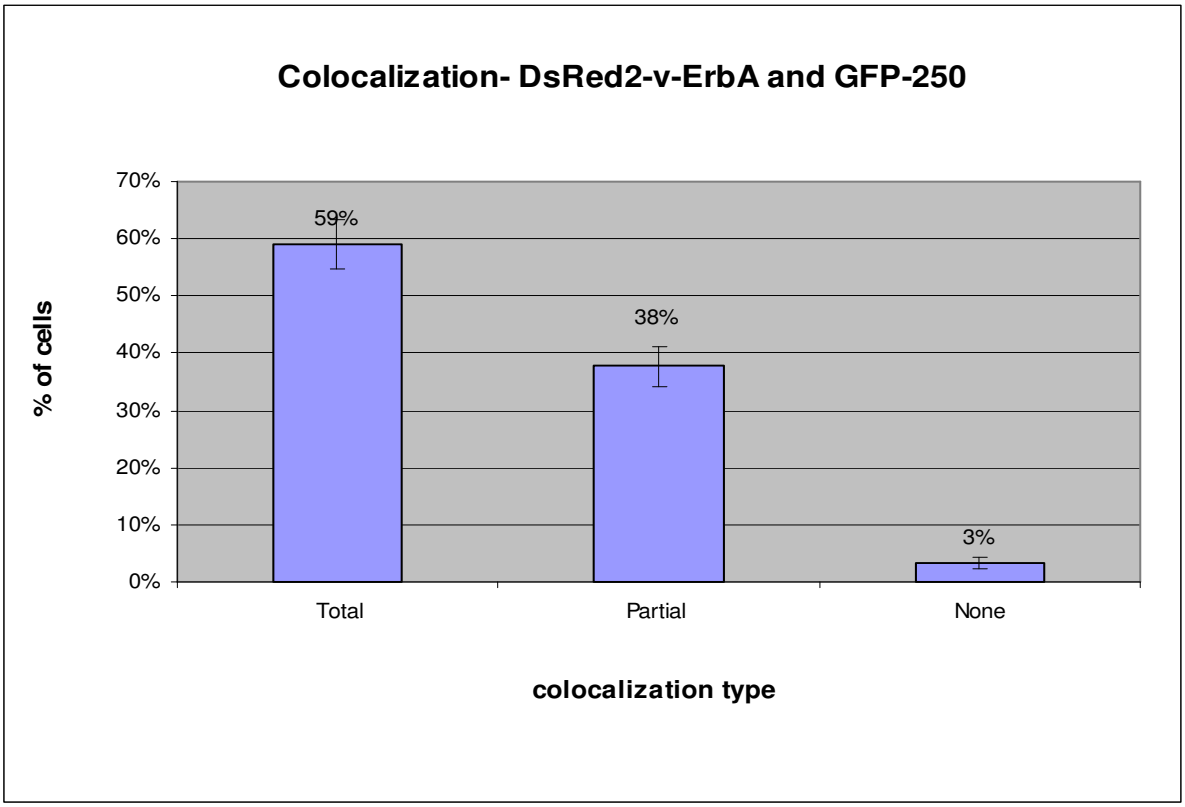

Figure 8: Colocalization statistics- GFP-250 and DsRed2-v-ErbA

Forty-eight hours after transfection, DsRed2-v-ErbA and GFP-250 completely colocalized in 59 ± 4% of cells and partially colocalized in 38 ± 4% of cells (n=3 replicate transfections, 313 cells scored). Error bars indicate SEM.

Cells were fixed both 48 hours (Figure 7) and 24 hours (Figure 9) post-transfection to observe the dynamics of aggresome formation. After 24 hours, cells cotransfected with DsRed2-v-ErbA and GFP-250 contained smaller more dispersed aggregates of both proteins throughout the cytoplasm. There was a high degree of colocalization between these small aggregates (Figure 9), suggesting that both of these proteins follow the same dynamic pathway. Over time, v-ErbA aggregates are transported via microtubule motors and coalesce at the MTOC. After 48 hours, the cells contained larger coalesced aggregates of both GFP-250 and DsRed2-v-ErbA (Figure 7). Additionally, DsRed2-v-ErbA colocalized with the cytoplasmic aggregates formed by the aggresomal marker GFP-170 (Figure 10). Taken together, these data provide strong evidence for association of v-ErbA with aggresomes.

Since DsRed2-v-ErbA behaved in the same fashion when expressed individually and coexpressed with GFP-tagged aggresomal markers (compare Figure 6 with Figures 7, 9, and 10), the possibility that the aggregation is caused by an interaction between fluorescent tags on these two proteins can be eliminated. In addition, prior studies have shown that untagged v-ErbA also forms aggregates (Bonamy et al., 2005).

Formation of v-ErbA foci is microtubule-dependent

After demonstrating that v-ErbA colocalized with aggresomal markers, it was necessary to investigate whether v-ErbA foci possessed defining aggresomal characteristics. Formation of

(a)

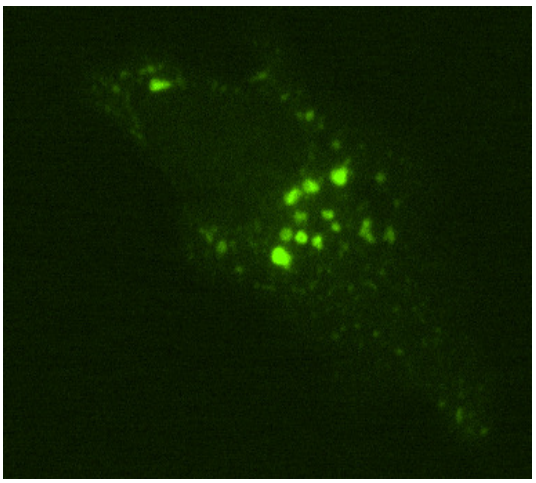

(b)

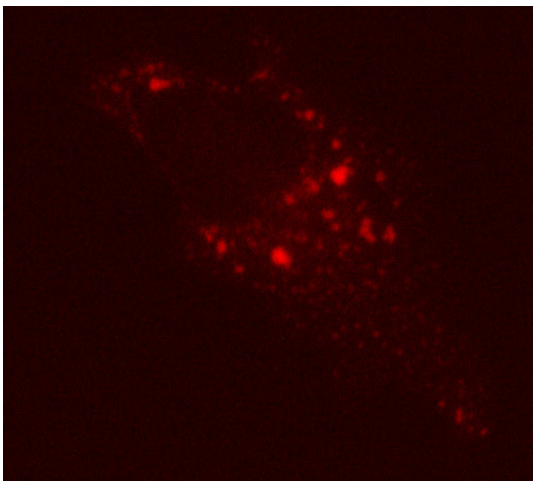

(c)

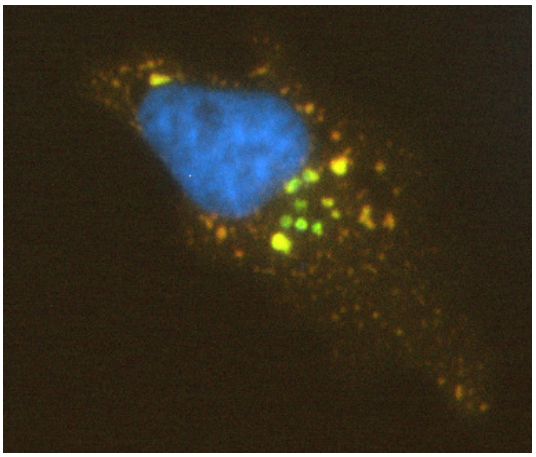

Figure 9: **Colocalization of the aggresomal marker GFP-250 and DsRed2-v-ErbA (24 hours post-transfection)**

(a) Subcellular distribution of GFP-250 (green)
(b) Subcellular distribution of DsRed2-v-ErbA (red)
(c) Merge of GFP-250 and DsRed2-v-ErbA. Yellow indicates colocalization between GFP-250 and DsRed2-v-ErbA. Nuclei were stained with DAPI (blue).

(a)

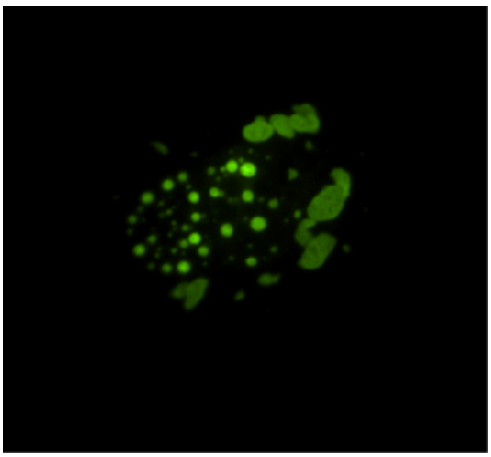

(b)

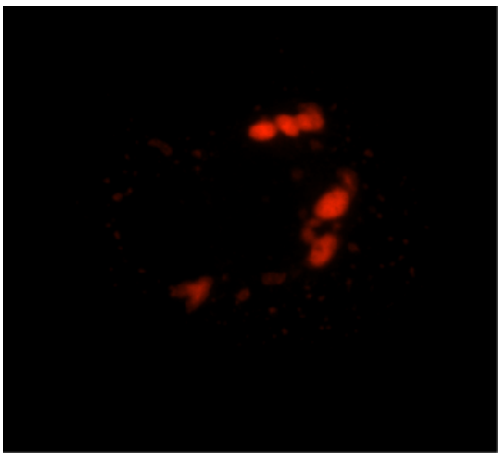

(c)

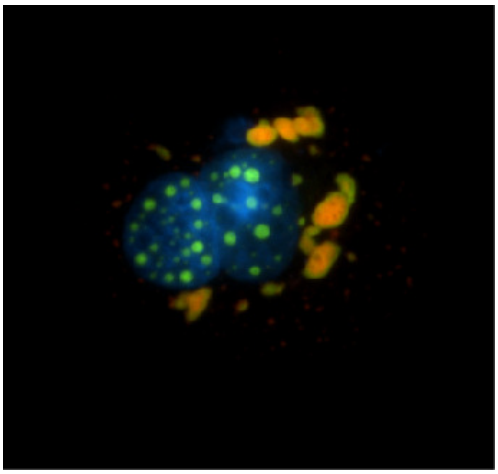

Figure 10: Colocalization of the aggresomal marker GFP-170 and DsRed2-v-ErbA (48 hours post-transfection)

(a) Subcellular distribution of GFP-170 (green)
(b) Subcellular distribution of DsRed2-v-ErbA (red)
(c) Merge of GFP-170 and DsRed2-v-ErbA. Yellow indicates colocalization between GFP-250 and DsRed2-v-ErbA. Nuclei were stained with DAPI (blue)

the aggresome requires transport of smaller aggregated proteins along microtubules. Thus, microtubule disruption prevents aggresome formation.

If the cytoplasmic foci formed by v-ErbA are a result of targeting to aggresomes, then microtubule inhibition would prevent the formation of these large, coalesced structures. To determine whether the disruption of microtubules would prevent the formation of the coalesced foci, HeLa cells expressing GFP-v-ErbA were treated with nocodazole for 20 hours (starting 16 hours post-transfection). Nocodazole disrupts microtubules by preventing their polymerization. The drug binds to a sulfhydryl group on β-tubulin and prevents disulfide linkages with additional tubulin heterodimers (Luduena and Roach, 1991; Vasquez et al., 1997). Microtubule disruption inhibits transport of cargo and cell division (Luduena and Roach, 1991).

If aggresome formation was inhibited, one would expect to see a diffuse expression pattern or a dispersal of small aggregates throughout the cytoplasm. As predicted, treatment of GFP-v-ErbA- expressing cells with nocodazole resulted in mostly cells with a diffuse pattern of v-ErbA expression (Figure 11). Only 13 ± 3% of untreated cells (n=2 replicate transfections, 200 cells scored) contained diffuse aggregates (Figure 12). Upon nocodazole treatment, there was a significant shift ($p < 0.001$) to 55 ± 3% of cells containing diffuse aggregates (Figure 12).While 46 ± 5% of untreated v-ErbA-expressing cells contained large aggregates, only 7 ± 3% of nocodazole-treated cells had large aggregates (Figure 12). Because nocodazole cannot disrupt aggregates that are already intact prior to treatment, many of the aggregates observed

(a)

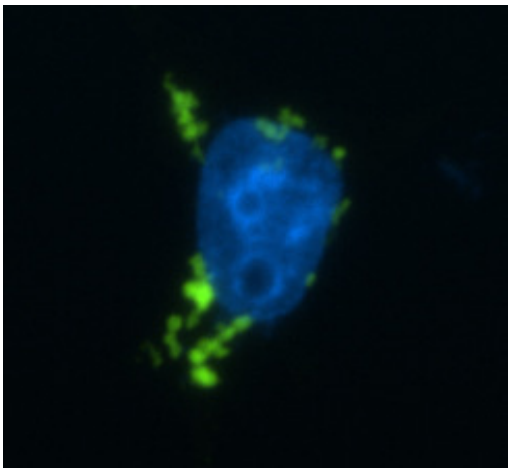

(b)

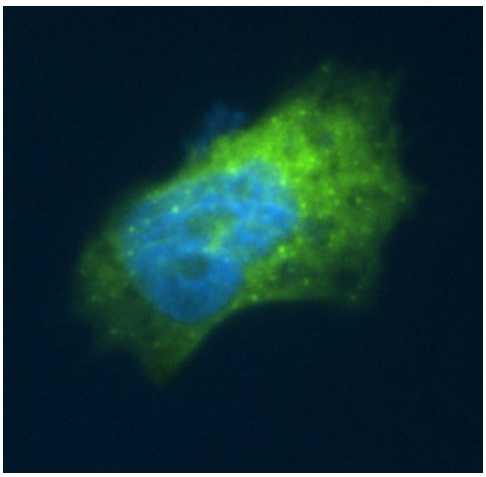

(c)

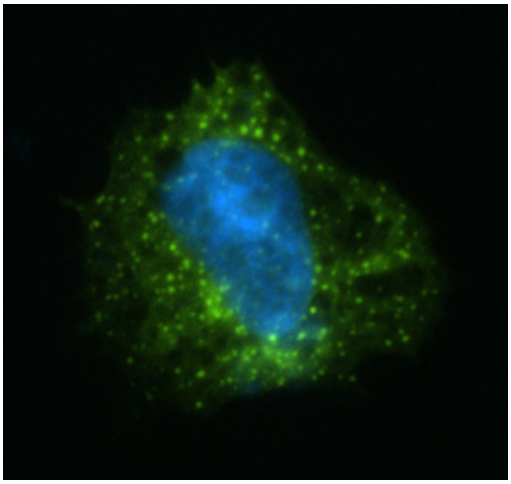

Figure 11: Formation of v-ErbA foci is microtubule-dependent

To determine whether the disruption of microtubules would prevent the formation of the coalesced foci, cells expressing GFP-v-ErbA were treated with nocodazole for 20 hours (starting 16 hours post-transfection). Nuclei were stained with DAPI (blue).

(a) Untreated cell forming large juxtanuclear foci.
(b) Nocodazole-treated cell forming diffuse aggregates
(c) Nocodazole-treated cell forming small aggregates, uniform in size.

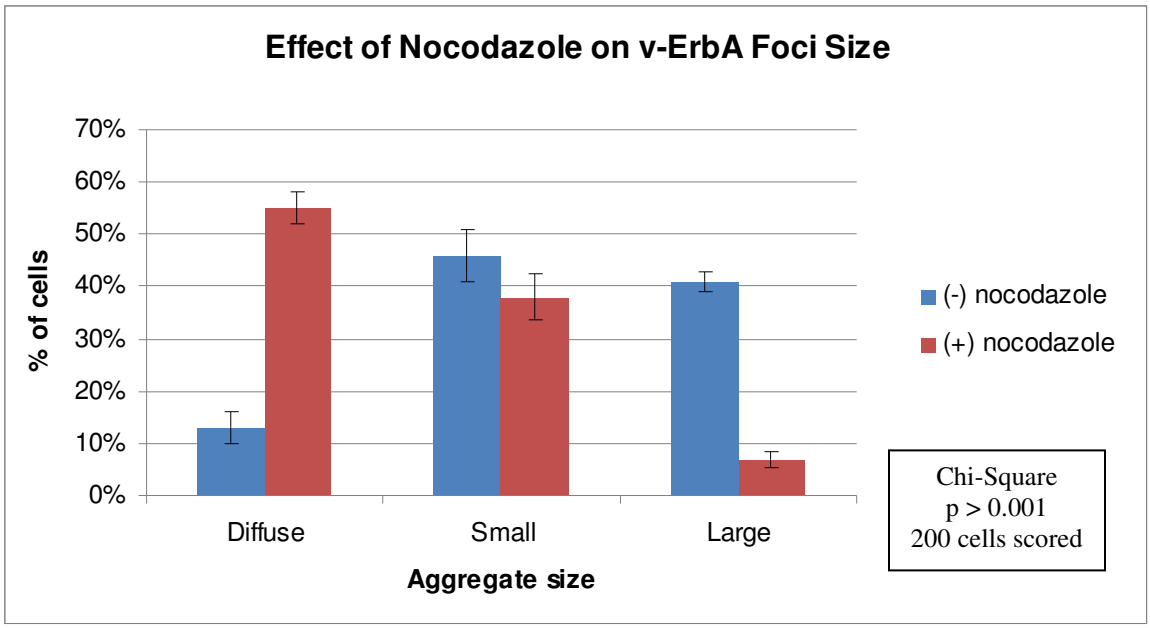

Figure 12: Effect of nocodazole on v-ErbA foci size

Upon nocodazole treatment, there was a significant shift ($P < 0.001$) in frequency distribution from larger foci to smaller, more diffuse foci. Error bars indicate SEM.

in treated cells could have been preexisting. Data thus suggest that over time, v-ErbA aggregates are transported via microtubule motors and coalesce at the MTOC.

Proteasome inhibition enhances the size of v-ErbA foci

Proteasome inhibition leads to an increase in aggresome size (Johnston et al., 1998; Garcia-Mata et al., 1999; Fu et al., 2005). The inhibition of proteasome activity leads to an increase in protein that would normally be degraded, leading to an accumulation of aggregated protein peripherally, which is transported to the MTOC. To determine whether the size of v-ErbA foci would increase in response to proteasome inhibition, cells expressing GFP-v-ErbA were treated with the proteasome inhibitor MG132 for 20 hours (starting 16 hours post-transfection). MG132 inhibits proteasome degradation by inhibiting the chymotrypsin-like activity of the proteasome, preventing the cleavage of peptide bonds within the protein of interest (Lee and Goldberg, 1998).

As predicted, MG132 treatment increased the size v-ErbA foci. Only 41 ± 2% (n=2 replicate transfections, 200 cells scored) of untreated cells contained large aggregates of GFP-v-ErbA, but upon MG132 treatment, there was a significant shift ($p > 0.001$) to 78 ± 7% of v-ErbA-expressing cells containing large aggregates (Figure 13). Interestingly, most of the large aggregates were spherical in morphology and coalesced into a single aggregate (Figure 13b), similar to the spherical aggregates formed by GFP-250, mutant huntingtin (Kuemmerle et al., 1999) and cystic fibrosis transmembrane regulator (Johnston et al., 1998) after proteasome

(a)

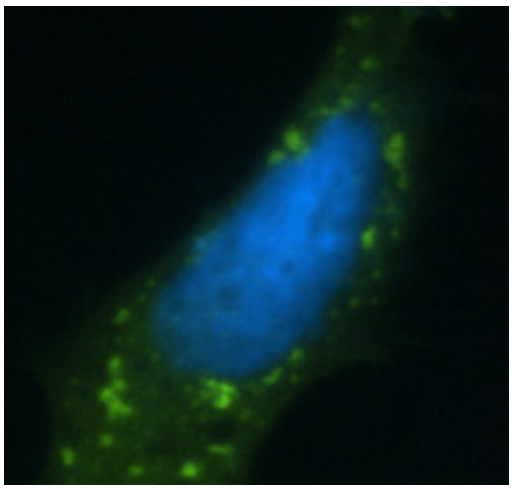

(b)

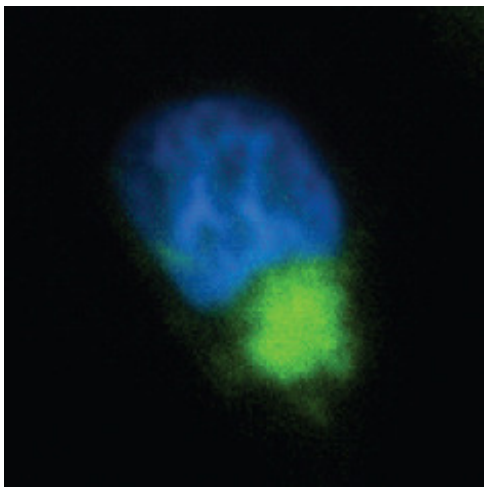

(c)

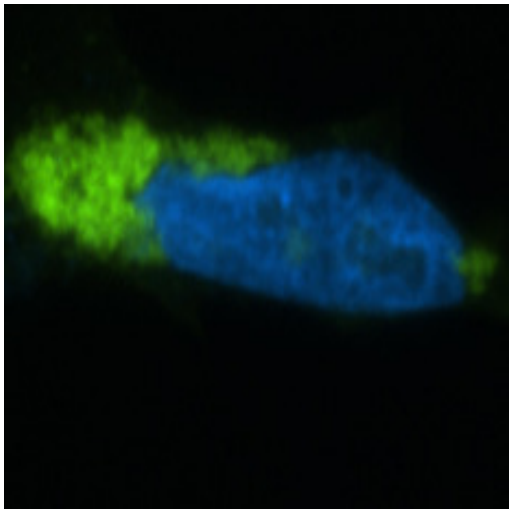

(d)

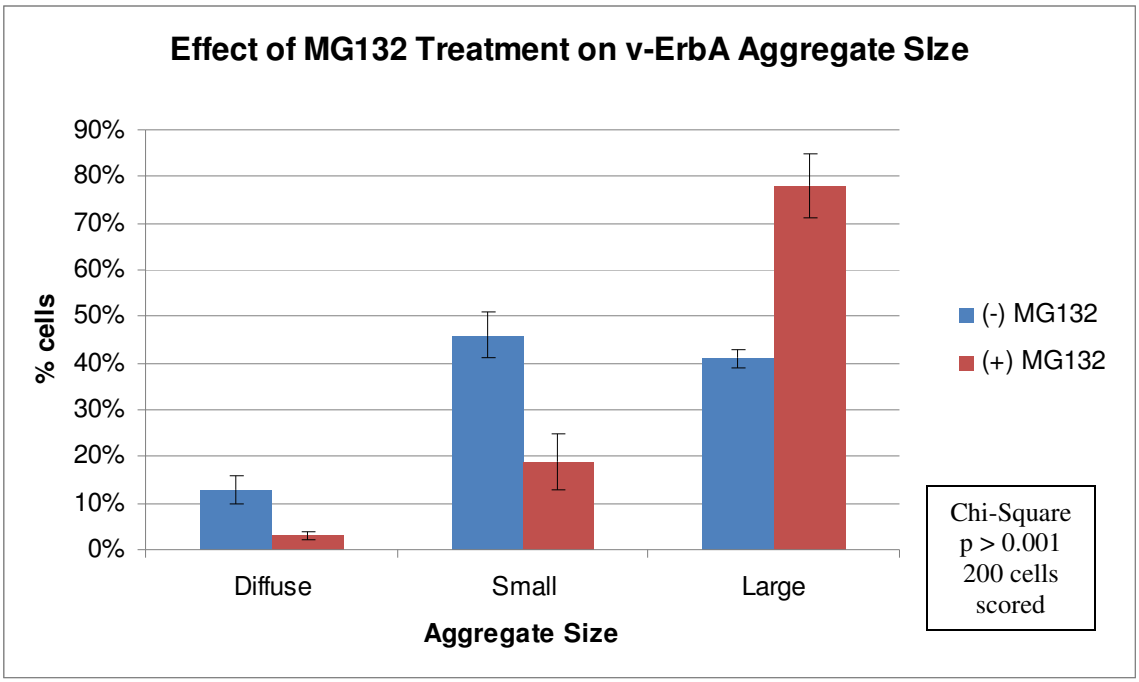

Figure 13: Effect of MG132 treatment of v-ErbA aggregate size

To determine whether the size of v-ErbA foci would increase in response to proteasome inhibition, cells expressing GFP-v-ErbA were treated with the proteasome inhibitor MG132 for 20 hours (16 hours post-transfection).

(a) Untreated v-ErbA expressing cell.
(b) MG132-treated v-ErbA expressing cell. Most of the large aggregates were spherical in morphology and coalesced into a single aggregate.
(c) MG132-treated v-ErbA expressing cell. Some of the large aggregates had a more undefined morphology (less common).
(d) Statistical analysis. Upon nocodazole treatment, there was a significant shift ($p < 0.001$) in frequency distribution from smaller aggregates to large aggregates. Error bars indicate SEM.

inhibition. This morphology is not observed in v-ErbA foci in the absence of proteasome inhibition. In addition, a few of the large aggregates had a more undefined morphology (Figure 13c). Taken together, these results suggest that the proteasome machinery normally degrades some of the aggregated v-ErbA, thus preventing aggresome formation.

v-ErbA foci disrupt vimentin intermediate filaments

Aggresomes are known to disrupt the intermediate filament meshwork composed of vimentin (Johnston et al. 1998, Garcia-Mata et al. 1999, Fu et al., 2005). To determine whether v-ErbA foci caused a disruption of vimentin, cells transfected with GFP-v-ErbA were stained with a Cy3-conjugated antibody against vimentin 48 hours post-transfection. In untransfected cells, the vimentin distribution pattern was filamentous and dispersed throughout the cell (Figure 14). However, cells transfected with GFP-v-ErbA showed a reorganization and collapse of vimentin filaments around the area of aggregated protein (n=3 replicate transfections, > 300 cells scored) (Figure 14). The same vimentin disruption was observed around the cytoplasmic aggregates formed by the aggresomal marker GFP-170 (Figure 15). These results provide additional evidence that v-ErbA foci exhibit aggresomal characteristics.

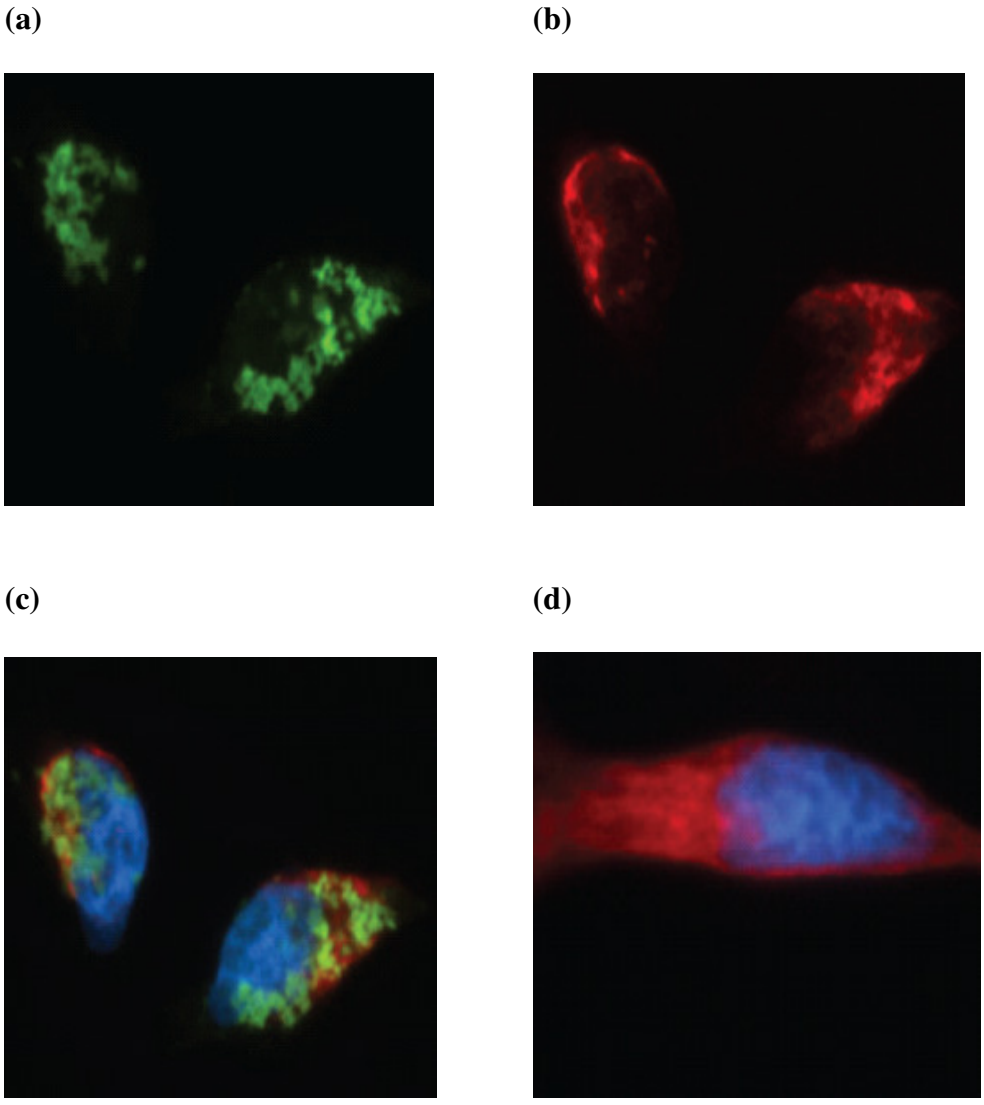

Figure 14: v-ErbA foci disrupt vimentin intermediate filaments

To determine whether v-ErbA foci caused a disruption of vimentin filaments, cells transfected with GFP-v-ErbA were stained with a Cy3-conjugated antibody against vimentin 48 hours post-transfection. (n=3, > 300 cells scored)

(a) Distribution of GFP-v-ErbA (green)
(b) Distribution of Cy3-conjugated antibody against vimentin (red)
(c) Merged image of GFP-v-ErbA and Cy3-vimentin. Nuclei stained with DAPI (blue). Cells transfected with GFP-v-ErbA showed a reorganization and collapse of vimentin around the area of aggregated protein.
(d) In untransfected cells, the vimentin distribution pattern was filamentous and dispersed throughout the cell. Nuclei stained with DAPI (blue).

(a)

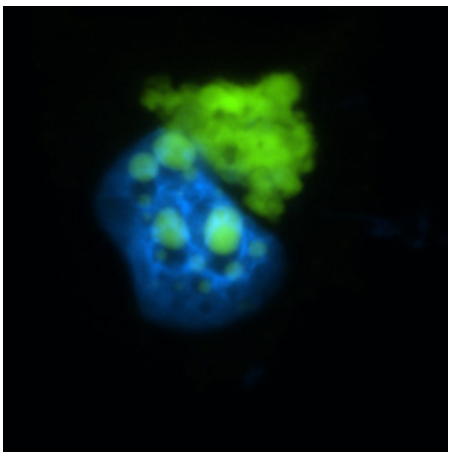

(b)

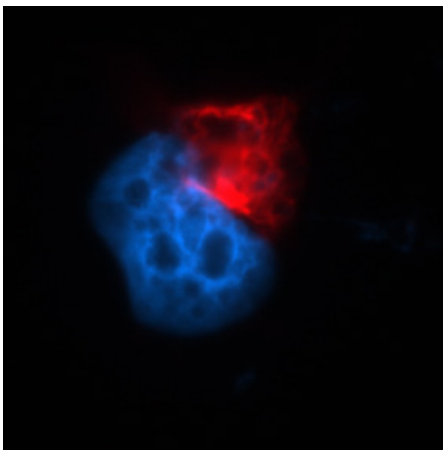

(c)

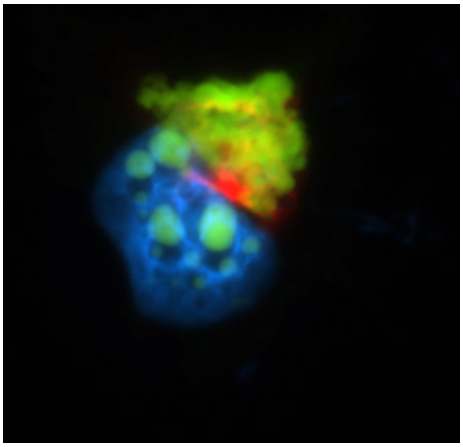

Figure 15: The cytoplasmic aggregates formed by GFP-170 disrupt vimentin intermediate filaments

(a) GFP-170 (green) distribution in relation to the DAPI-stained nucleus (blue).
(b) Cy3-vimentin distribution (red). Nucleus stained with DAPI (blue)
(c) Merged image of GFP-170 and Cy3-vimentin. Cells transfected with GFP-170 showed a reorganization and collapse of vimentin around the cytoplasmic aggregates. A very similar disruption pattern was observed around GFP-v-ErbA aggregates (See Figure 14).

Discussion

v-ErbA, an oncoprotein derived from the avian erythroblastosis virus (AEV), mislocalizes to cytoplasmic foci and sequesters the thyroid hormone receptor (TR) in these foci, contributing to its oncogenic properties (Bonamy et al., 2005). This thesis research provides strong evidence that cytoplasmic mislocalization of v-ErbA is a result of targeting to aggresomes, either for turnover of misfolded protein or for viral replication and assembly. v-ErbA foci colocalized with aggresomal markers, were dependent on microtubule transport for their formation, were enhanced in size upon treatment with proteasome inhibitors, and disrupted the intermediate filament meshwork composed of vimentin. These results indicate an association between v-ErbA foci and aggresomes.

Dynamics and morphology of v-ErbA foci

While all aggresome-forming proteins follow similar dynamics, the final morphology of the aggresome is variable. However, aggresome formation is generally categorized into two broad categories: spherical or ribbon-like (Garcia-Mata et al., 2002). Spherical aggresomes are formed by mutant huntingtin (Kuemmerle et al., 1999), mutant cystic fibrosis transmembrane conductance regulator (CFTR) (Johnston et al., 1998), and the aggresomal marker GFP-250 (Garcia-Mata et al., 1999). However, it is important to note that the spherical aggresomes formed by CFTR are induced by proteasome inhibitors (Johnston et al., 1998). Additionally, many viral particles that follow the aggresomal pathway have a

spherical morphology, evidenced by African Swine Fever Virus (ASFV) particles (Heath et al., 2001). Ribbon-like aggresomes can be formed by UCH-L1 in Parkinson's (Ardley et al., 2004), glial fibrillary protein (GFAP) in Alexander's Disease (Mignot et al., 2007), ATP7B in Wilson's disease (Harada et al., 2001), and the aggresomal marker GFP-170 (Fu et al., 2005). The criteria for formation of either of these two distinct morphologies have yet to be determined.

v-ErbA foci appear to form the ribbon-like shape seen in the cytoplasmic aggregates formed by GFP-170, but are still very similar to the aggregates formed by GFP-250, which can be more spherical in shape. Forty-eight hours post-transfection, the foci formed by DsRed2-tagged-v-ErbA completely colocalized with GFP-250 in 59 ± 4% of cells and partially colocalized with GFP-250 in 38 ± 4% of cells. The number of cells exhibiting complete colocalization between v-ErbA and GFP-250 is somewhat higher than expected, since the two proteins differ in final morphology. These results suggest that the final aggresomal morphology is not always reached after 48 hours. Additionally, the results indicate that the two proteins undergo the same dynamics, which is evidenced by the colocalization of smaller aggregates formed by both v-ErbA and GFP-250 observed 24 hours post-transfection.

Microtubule-dependent formation

Disruption of microtubules with nocodazole yielded small, dispersed aggregates of v-ErbA throughout the cytoplasm and prevented the coalescence of protein into a large aggregate at the microtubule organizing center. Likewise, both misfolded proteins and viral particles are

dependent on microtubule transport for aggresome formation (Johnston et al., 1998; Garcia-Mata et al., 1999; Heath et al., 2001). Thus, v-ErbA movement occurs by a microtubule motor-driven process.

Proteasome inhibition

Treatment with the proteasome inhibitor MG132 enhanced the size of v-ErbA foci, which was as predicted. Interestingly, the vast majority of the large aggregates coalesced into a large, spherical structure. This shape was similar to the aggregates formed by GFP-250, mutant huntingtin (Kuemmerle et al., 1999) and cystic fibrosis transmembrane regulator after proteasome inhibition. This spherical morphology is not observed in v-ErbA foci in the absence of proteasome inhibition. Because MG132 treatment speeds up the kinetics of aggresome formation, the final shape of the aggresome can be reached more quickly, which could explain why this spherical shape was not reached in untreated cells. Regardless, it is evident from these results that protein degradation by the proteasome is critical for clearance of v-ErbA from the cell.

Reorganization of vimentin

A number of aggresome-forming misfolded proteins and viral particles have been shown to cause a collapse of vimentin filaments into a circular “cage” around the area of aggregated protein for immobilization and containment (Johnston et al., 1998; Garcia-Mata et al., 1999; Heath et al., 2001). This is only seen in aggresomes with a spherical morphology. Since v-

ErbA has a more ribbon-like morphology (in the absence of proteasome inhibition), the formation of a circular "cage" around the area of aggregated protein was not expected. The vimentin disruption pattern in v-ErbA-expressing cells was very similar to the disruption pattern around the cytoplasmic aggregates formed by the aggresomal marker GFP-170. However, it would be interesting to determine whether the vimentin collapsed in a cage-like formation in v-ErbA-expressing cells that were treated with proteasome inhibitors, since proteasome inhibition with MG132 caused v-ErbA to form a large and spherical aggregate.

Significance of targeting of v-ErbA to aggresomes- mechanism of turnover

The results presented here indicate an association between cytoplasmic v-ErbA foci and aggresomes. One possible explanation for targeting of the oncoprotein v-ErbA to aggresomes is to sequester the protein for turnover and disposal, preventing its dominant negative activity on TR in the nucleus. If turnover of v-ErbA does in fact occur after the aggregates coalesce at the microtubule-organizing center (MTOC), it is necessary to investigate the specific mechanisms by which v-ErbA could be degraded.

First, the aggregates might by degraded by proteasome machinery. However, proteasome degradation might not be very efficient at the aggresome (Garcia-Mata et al., 2002). Second, the aggregates might undergo autophagic clearance. Proteasome degradation could be dominant in the turnover of v-ErbA, autophagy could be dominant, or the two systems could contribute equally. It is important to investigate the efficiency of v-ErbA degradation promoted by both the proteasome and autophagy. It has been suggested that proteasome

degradation might not be very efficient at the aggresome (Garcia-Mata et al., 2002). Instead, autophagy might be a more effective system for degradation because the process allows large portions of cytoplasm containing aggregated proteins to be engulfed in an isolation membrane and targeted to the lysosome for degradation. Regardless, either of these pathways could become saturated after an accumulation of a certain amount of aggregated protein. Therefore, there could be limits to how much protein degradation can be induced in response to aggresome formation, regardless of the mechanisms. Cells might simply undergo apoptosis after the accumulation of a specific amount of aggregated protein, evidenced in cells containing glial fibrillary acidic protein (GFAP) aggregates (Mignot et al., 2007).

Significance of targeting of v-ErbA to aggresomes- remnant viral behavior for assembly

Another possible explanation for the association of cytoplasmic v-ErbA foci with aggresomes could be a remnant viral behavior for assembly, exploiting the aggresomal pathway for the turnover of misfolded protein. Aggresome-forming viral factories have been shown to colocalize with the aggresomal marker GFP-250, disrupt vimentin intermediate filaments, and depend on intact microtubules for their formation, consistent with the properties of v-ErbA foci (Heath et al., 2001). The retroviral oncoprotein v-ErbA is a fusion protein that contains a portion of the retroviral Gag sequence, which encodes structural proteins involved in the formation of the viral capsid. It is not known whether or not the Gag sequence itself is recognized by dynein motors, resulting in its transport to the MTOC. Therefore, further studies could investigate the role of the Gag sequence in its aggresomal behavior by investigating the effects of Gag deletion. Prior studies in our lab have shown that

the Gag portion of v-ErbA mediates CRM1-dependent nuclear export (DeLong et al., 2004). Deletion of the v-ErbA Gag sequence resulted in a more nuclear localization. The functional role of Gag-mediated nuclear export of v-ErbA is unknown, but the results in this thesis support the hypothesis that it could be a remnant behavior of viral assembly by targeting of v-ErbA to aggresomes.

General questions about the aggresome

There are a number of remaining questions about the aggresome. Although aggresome formation by mutant proteins involved in neurodegenerative disorders and viral proteins is well characterized, it is still not certain whether the aggresome is a general response to the accumulation of aggregates caused by misfolded protein. To determine whether the aggresome is a general response to misfolded protein, it is necessary to study aggresome formation in more non-neurodegenerative disease systems.

Interestingly, aggresome formation is induced by a mutant of the androgen receptor (AR) (Taylor et al., 2003), which is a member of the nuclear receptor subfamily along with the thyroid hormone receptor (TR). However, it contains polyglutamine expansions and is associated with spinobulbar muscular atrophy, a neurodegenerative disease. Therefore, the AR mutant has very similar properties to the vast majority of aggresome-forming proteins that have been studied and does not provide much insight into the nature of aggregation of mutant proteins within the nuclear receptor family, specifically mutants of TR.

The association of aggresome formation with signaling pathways is also poorly understood. For example, it is unclear what signaling pathways accompany the recruitment of proteasome machinery, chaperone proteins, and mitochondria to the aggresome. Further insight into these pathways could help find ways to induce and amplify degradation mechanisms, specifically proteasome degradation and autophagy.

Are aggresomes pathogenic or cytoprotective?

Aggresome formation has been described to have pathogenic consequences. Studies in transgenic mice have shown that the expression of a mutant huntingtin protein forms aggresomes in a number of neurons, correlating with neurodegeneration and symptoms of Huntington's disease (Lin et al., 2001). Additionally, aggresomes formed by cytokeratin proteins in alcoholic liver disease have been shown to correlate with cell death (Nakamichi et al., 2002). However, this may have to do with the unavailability of functional protein and not the aggresome itself.

The aggresome could contribute to pathogenesis for a number of reasons. First, the aggresome recruits a great deal of the proteasome and chaperone machinery in the cell and saturates the autophagic pathway. This would certainly have to cause detriment to the cell eventually because other proteins in the cell would fail to be degraded; proto-oncogene products would accumulate, disrupting cell cycle regulation. Second, the collapse of the vimentin around the aggresome might make the rest of the cell vulnerable to mechanical stress, since vimentin plays a structural role in the cell. Additionally, other organelles in the

cell might not be anchored appropriately due to the vimentin redistribution. Third, formation of the aggresome might saturate dynein motors and lead to disrupted transport of organelles and other cargo.

In contrast, a number of studies have described aggresome formation as cytoprotective. Formation of this structure resulted in reduced levels of mutant Huntington and a decrease in neurodegeneration (Arrasate et al., 2004; Iwata et al., 2005). Aggresome formation is also associated with reduced cytotoxicity in cellular models containing mutants of peripheral myelin protein 22 (PMP22), androgen receptor, and α-synuclein. (Fortun et al., 2003; Taylor et al., 2003; Tanaka et al., 2004).

In conclusion, the aggresome seems to correlate with pathogenesis because of the unavailability of functional protein, not because the aggresome itself is pathogenic. Formation of the aggresome facilitates the turnover of aggregated protein, protecting cells from consequences of the accumulation of dispersed cytoplasmic aggregates. The aggresome might be an efficient temporary solution to the accumulation of aggregated protein, but it might not be cytoprotective if proteasome machinery and autophagic pathways become saturated.

If the association of v-ErbA and aggresomes is a result of sequestering v-ErbA for protein turnover, formation of the aggresome appears to be cytoprotective in this situation.

Formation of the aggresome would protect cells from the pathogenic consequences of an accumulation of v-ErbA aggregates dispersed throughout the cytoplasm. Additionally, aggresome formation would protect cells from the dominant negative activity of v-ErbA on TR in the nucleus. However, aggresome formation by v-ErbA could also have pathogenic consequences because v-ErbA can sequester TR in its cytoplasmic foci, preventing TR from regulating transcription of its target genes, adding to its dominant negative activity (Bonamy et al., 2005; Bonamy and Allison, 2006).

Future directions

First, to confirm and extend the findings of this thesis research, it is necessary to provide additional evidence that v-ErbA foci possess aggresomal characteristics. This can be explored by testing the association of v-ErbA foci with proteasome subunits, chaperone proteins, ubiquitin, the microtubule organizing center (gamma-tubulin), dynein and adaptor proteins (dynactin and HDAC6), and markers of autophagy, primarily by using antibodies against these components. These studies would not only strengthen the hypothesis of an association between v-ErbA and aggresomes, but would also provide insight into the fate of v-ErbA after its sequestration. For example, a strong association with ubiquitin and proteasome subunits would suggest that v-ErbA foci undergo proteasome degradation, and a strong association with autophagic markers would suggest that v-ErbA is targeted to the lysosome for degradation. If there is an association between v-ErbA foci and proteasome

subunits or autophagic markers, it would be necessary to investigate the efficiency of these turnover mechanisms.

The cellular fate of v-ErbA after localization to the aggresome can also be investigated by tagging it with a photoactivatable fluorescent protein (PAFP). Future studies in our lab will tag v-ErbA with Dendra, a PAFP derived from the octocoral *Dendronephthya*, which undergoes laser-induced photoconversion from green to red fluorescence (Gurskaya et al., 2006). Therefore, the cellular localization of v-ErbA can be determined both before and after photoactivation, induced after v-ErbA has localized to the aggresome. These studies will provide insight into whether specific, photoactivated v-ErbA foci enlarge, are degraded, or migrate to another subcellular compartment, such as the nucleus, after aggresome formation.

Preliminary studies in our lab have demonstrated that the formation of v-ErbA foci; thus, aggresome formation, is partially reversible. Because v-ErbA is a shuttling protein, it is contained in the nucleus when export is blocked. When treated with the drug leptomycin B (LMB), which inhibits CRM1-mediated nuclear export, smaller cytoplamic v-ErbA foci have been shown to disappear and apparently accumulate in the nucleus. However, large cytoplasmic foci formed by v-ErbA do not appear to undergo disassociation and remain cytoplasmic.

In conclusion, the results presented in this thesis and future studies will all provide insight into the viral oncoprotein v-ErbA and its associations with aggresomal pathways, either for protein turnover or viral assembly. Additionally, more knowledge can be gained concerning

the fate of TR after its mislocalization to the cytoplasm by v-ErbA, and the role this plays in oncogenesis. Finally, these studies contribute to a general understanding of the aggresome and its role in pathogenesis and turnover of misfolded proteins.

References

Arnaud F, Murcia P, and Palmarini, M. Mechansims of late restriction induced by an endogenous virus. J Virol. 2007; 81: 11441-51.

Arrasate M, Mitra S, Schweitzer ES, Segal MR, Finkbeiner S. Inclusion body formation reduces levels of mutant huntingtin and risk of neuronal cell death. Nature 2004; 431: 805–10.

Bonamy GM, Guiochon-Mantel A, Allison LA. Cancer promoted by the oncoprotein v-ErbA may be due to subcellular mislocalization of nuclear receptors. Mol Endocrinol 2005; 19: 1213-1230.

Braliou GG, Ciana P, Klaassen W, Gandrillon O, Stunnenberg HG. The v-ErbA oncoprotein quenches the activity of an erythroid-specific enhancer. Oncogene 2001; 20: 775–787.

Bunn CF, Neidig JA, Freidinger KE, Stankiewicz TA, Weaver BS, McGrew J, Allison LA. Nucleocytoplasmic shuttling of the thyroid hormone receptor α. Mol Endocrinol 2001; 15: 512-33.

Campbell RE, Tour O, Palmer AE, Steinbach PA, Baird GS, Zacharias DA, Tsien RY. A monomeric red fluorescent protein. Proc Natl Acad Sci USA 2002; 99: 7877-82.

DeLong LJ, Bonamy GM, Fink EN, Allison LA. Nuclear export of the oncoprotein v-ErbA is mediated by acquisition of a viral nuclear export sequence. J Biol Chem. 2004; 279: 15356-67.

Fabunmi RP, Wigley WC, Thomas PJ, DeMartino GN. Activity and regulation of the centrosome-associated proteasome. J Biol Chem 2000; 275: 409–413.

Fabbro, M. and Henderson, B. Regulation of tumor suppressors by nuclear-cytoplasmic shuttling. Exp. Cell Res. 1003; 282: 59–69.

Fortun J, Dunn W, Joy S, Li J, and Notterpek L. Emerging role for autophagy in the removal of aggresomes in Schwann cells, J. Neurosci. 23; 2003:10672–10680.

Fu L, Gao YS, Tousson A, Shah A, Chen TL, Vertel BM, Sztul E. Nuclear Aggresomes Form by Fusion of PML-associated Aggregates. Mol Biol Cell. 2005; 16:4905-4917.

Garcia-Mata R, Bebok Z, Sorscher EJ, Sztul ES. Characterization and dynamics of aggresome formation by a cytosolic GFP-chimera. J Cell Biol 1999; 146:1239-1254.

Garcia-Mata R, Gao YS, Sztul E. Hassles with taking out the garbage: aggravating aggresomes. Traffic 2002; 3: 388-96.

Grespin, M.E., Bonamy, G.M., Cameron, N.G., Adam, L.E., Atchison, A.P., Fratto, V.M., Allison, L.A. Thyroid hormone receptor α1 follows a cooperative CRM1/calreticulin-mediated nuclear export pathway. Journal of Biological Chemistry 2008, *under revision*.

Gurskaya NG, Verkhusha VV, Shcheglov AS, Staroverov DB, Chepurnykh TV, Fradkov AF, Lukyanov S, Lukyanov KA. Engineering of a monomeric green-to-red photoactivatable fluorescent protein induced by blue light. Nat Biotechnol. 2006; 24: 461-5.

Harada M, Sakisaka S, Terada K, Kimura R, Kawaguchi T, Koga H, Kim M, Taniguchi E, Hanada S, Suganuma T, Furuta K, Sugiyama T, Sata M. A mutation of the Wilson disease protein, ATP7B, is degraded in the proteasomes and forms protein aggregates. Gastroenterology 2001;120: 967–974.

Heath CM, Windsor M, Wileman T. Aggresomes resemble sites specialized for virus assembly. J. Cell Biol. 2001; 153: 449–56.

Hicks, S. W., and Machamer, C. E. The NH2-terminal domain of Golgin-160 contains both Golgi and nuclear targeting information. J. Biol. Chem. 2002; 277: 35833-35839.

Iwata A, Riley B, Johnston J and Kopito R. HDAC6 and microtubules are required for autophagic degradation of aggregated huntingtin, J. Biol. Chem. 280; 2005:40282–40292.

Johnston JA, Ward CL, Kopito RR. Aggresomes: A cellular response to misfolded proteins. J Cell Biol 1998; 143: 1883-1898.

Klionsky DL. The molecular machinery of autophagy: unanswered questions. J. Cell Sci. 2005; 118: 7–18.

Kuemmerle S, Gutekunst CA, Klein AM, Li XJ, Li SH, Beal MF, Hersch SM, Ferrante RJ. Huntington aggregates may not predict neuronal death in Huntington's disease. Ann Neurol 1999; 46: 842–849.

Lee, D.H., and Goldberg, A.L., Proteasome inhibitors: valuable new tools for cell biologists. Trends Cell Biol. 1998; 8: 397-403.

Lin CH, Tallaksen-Greene S, Chien WM, Cearley JA, Jackson WS, Crouse AB, Ren S, Li XJ, Albin RL, Detloff PJ. Neurological abnormalities in a knock-in mouse model of Huntington's disease. Hum Mol Genet 2001; 10: 137-144.

Luduena, R.F., and Roach, M.C, Tubulin sulfhydryl groups as probes and targets for antimitotic and antimicrotubule agents. Pharmacol. Ther. 1991; 49: 133-152.

Masliah E, Rockenstein E, Veinbergs I, Mallory M, Hashimoto M, Takeda A, Sagara Y, Sisk A, Mucke L. Dopaminergic loss and inclusion body formation in alpha-synuclein mice: Implications for neurodegenerative disorders. Science 2000; 287: 1265–1269

Mignot C, Delarasse C, Escaich S, Della Gaspera B, Noé E, Colucci-Guyon E, Babinet C, Pekny M, Vicart P, Boespflug-Tanguy O, Dautigny A, Rodriguez D, Pham-Dinh D. Dynamics of mutated GFAP aggregates revealed by real-time imaging of an astrocyte model of Alexander disease. Exp Cell Res. 2007; 313: 2766-79.

Mittal S, Dubey D, Yamakawa K, Ganesh S. Lafora disease proteins malin and laforin are recruited to aggresomes in response to proteasomal impairment. Hum Mol Genet. 2007; 16:753-62.

Mortimore GE, Miotto G, Venerando R, Kadowaki M, Autophagy. Subcell Biochem 1996; 27: 93–135.

Muchowski PJ, Schaffar G, Sittler A, Wanker EE, Hayer-Hartl MK, Hartl FU. Hsp70 and hsp40 chaperones can inhibit self-assembly of polyglutamine proteins into amyloid-like fibrils. Proc Natl Acad Sci USA 2000; 97: 7841-7846.

Muchowski, P. J. , Ning, K. , D'Souza-Schorey, C. & Fields, S. Requirement of an intact microtubule cytoskeleton for aggregation and inclusion body formation by a mutant huntingtin fragment. Proc. Natl Acad. Sci. USA 2002; 99: 727–732.

Nagl SB, Nelson CC, Romaniuk PJ, Allison LA. Constitutive transactivation by the thyroid hormone receptor and a novel pattern of activity of its oncogenic homolog v-ErbA in Xenopus oocytes. Mol Endocrinol. 1995; 9: 1522-32.

Nakamichi I, Hatakeyama S, and Nakayama K. Formation of Mallory body-like inclusions and cell death induced by deregulated expression of keratin 18, Mol. Biol. Cell 2002; 13: 3441–3451.

Nelson, D.S., Alvarez, C., Gao, Y.S., Garcia-Mata, R., Fialkowski, E., Sztul, E. The membrane transport factor TAP/p115 cycles between the Golgi and earlier secretory compartments and contains distinct domains required for its localization and function. J. Cell Biol. 1998: 143: 319-331

Nozawa N, Yamauchi Y, Ohtsuka K, Kawaguchi Y, Nishiyama Y. Formation of aggresome-like structures in herpes simplex virus type 2-infected cells and a potential role in virus assembly. Exp Cell Res; 2004; 299: 486-97.

Ross CA and Poirier MA. Protein aggregation and neurodegenerative disease. Nat Rev Mol Cell Biol. 2005; 6: 891-8.

Saliba RS, Munro PM, Luthert PJ, Cheetham ME. The cellular fate of mutant rhodopsin: quality control, degradation and aggresome formation. J Cell Sci. 2002; 115: 2907-18.

Stommel J. M., Marchenko N. D., Jimenez G. S., Moll U. M., Hope T. J., Wahl G. M. A leucine-rich nuclear export signal in the p53 tetramerization domain: regulation of subcellular localization and p53 activity by NES masking. Embo J. 1999; 18:1660–72.

Tanaka M, Kim Y, Lee G, Junn E, Iwatsubo T, Mouradian M. Aggresomes formed by α-synuclein and synphilin-1 are cytoprotective. J Biol Chem. 2004; 279: 4625-4631.

Taylor JP, Tanaka F, Robitschek J, Sandoval CM, Taye A, Markovic-Plese S, Fischbeck KH. Aggresomes protect cells by enhancing the degradation of toxic polyglutamine-containing protein. Hum Mol Genet; 2003: 749-757.

Thormeyer D, Baniahmad A. The v-erbA oncogene. Int J Mol Med. 1999; 4: 351-8.

Tsien, RY. The green fluorescent protein. Annu. Rev. Biochem. 1998; 67: 509-44.

Vasquez, RJ, Howell B, Yvon AM, Wadsworth P, Cassumeris L. Nanomolar concentrations of nocodazole alter microtubule dynamic instability in vivo and in vitro. Mol. Biol. Cell 1997; 8: 973-985.

Wigley WC, Fabunmi RP, Lee MG, Marino CR, Muallem S, DeMartino GN, Thomas PJ. Dynamic association of proteasomal machinery with the centrosome. J Cell Biol 1999; 145: 481-490.

Wileman T. Aggresomes and autophagy generate sites of virus replication. Science 2006; 312: 875–78.

Wojcik C, Schroeter D, Wilk S, Lamprecht J, Paweletz N. Ubiquitin-mediated proteolysis centers in HeLa cells: Indication from studies of an inhibitor of the chymotrypsin-like activity of the proteasome. Eur J Cell Biol 1996; 71: 311–318.

Zatloukal K, Stumptner C, Lehner M, Denk H, Baribault H, Eshkind LG, Franke WW. Cytokeratin 8 protects from hepatotoxicity, and its ratio to cytokeratin 18 determines the ability of hepatocytes to form Mallory bodies. Am J Pathol 2000; 156: 1263–1274.

Acknowledgements

A number of people contributed to the successful completion of this thesis research. First and foremost, Dr. Lizabeth Allison provided endless support, advice, and time throughout the last two years that she has supervised my research. Working in her laboratory has been an incredibly rewarding and enjoyable experience. I would also like to thank Dr. Eric Engstrom, Dr. Oliver Kerscher, and Dr. Lisa Landino for their advice, enthusiasm, and entertainment while serving on my thesis committee. Vinny and Molly Roggero assisted with statistical analyses of this thesis research. In addition, Vinny taught me a number of techniques when I first started working in the laboratory. Other members of the Allison laboratory, past and present, provided plasmids, assistance, and amusement throughout this thesis research. I couldn't have asked for a more delightful laboratory environment. Additionally, Elizabeth Sztul contributed plasmids essential for this research.

This thesis research was supported by a number of Student Research Grants and a Student Summer Research Fellowship Award, which were all funded by Howard Hughes Medical Institute grants through the Undergraduate Biological Sciences Education Program to the College of William and Mary. Additional funding was provided by a Mary E. Ferguson Memorial Research Grant through the College of William and Mary Biology department. Funding also came from grants to Dr. Allison from the National Science Foundation.

Appendix

Complete cell counts for colocalization- DsRed2-v-ErbA and GFP-250

	Total	Partial	None	# cells scored
Trial 1	75	34	2	111
Trial 2	54	43	5	102
Trial 3	57	40	3	100
Total	186	117	10	313

Complete cell counts- effect of nocodazole treatment on GFP-v-ErbA aggregate size

Chi-Square test- $p > 0.001$

	GFP-v-ErbA (untreated)	GFP-v-ErbA (nocodazole)
Diffuse, trial 1	16	58
Small, trial 1	41	33
Large, trial 1	43	9
Cells scored, trial 1	100	100
Diffuse, trial 2	10	52
Small, trial 2	51	42
Large, trial 2	39	6
Cells scored, trial 2	100	100
Diffuse, total	26	110
Small, total	92	75
Large, total	82	15
Cells scored, total	200	200

Complete cell counts- effect of MG132 treatment on GFP-v-ErbA aggregate size

Chi-Square test- $p > 0.001$

	GFP-v-ErbA (untreated)	GFP-v-ErbA (MG132)
Diffuse, trial 1	16	4
Small, trial 1	41	25
Large, trial 1	43	71
Cells scored, trial 1	100	100
Diffuse, trial 2	10	2
Small, trial 2	51	13
Large, trial 2	39	85
Cells scored, trial 2	100	100
Diffuse, total	26	6
Small, total	92	38
Large, total	82	156
Cells scored, total	200	200